ORGAN PHYSIOLOGY

Transport properties in CFTR−/− knockout piglets suggest normal airway surface liquid pH and enhanced amiloride-sensitive Na+ absorption

Roberta Benedetto[1] · Raquel Centeio[1] · Jiraporn Ousingsawat[1] · Rainer Schreiber[1] · Melanie Janda[2] · Karl Kunzelmann[1]

Abstract

Previous analysis of CFTR-knockout (CFTR−/−) in piglets has provided important insights into the pathology of cystic fibrosis. However, controversies exist as to the true contribution of CFTR to the pH balance in airways and intestine. We therefore compared ion transport properties in newborn wild-type (CFTR+/+) and CFTR-knockout (CFTR−/− piglets). Tracheas of CFTR−/− piglets demonstrated typical cartilage malformations and muscle cell bundles. CFTR−/− airway epithelial cells showed enhanced lipid peroxidation, suggesting inflammation early in life. CFTR was mainly expressed in airway submucosal glands and was absent in lungs of CFTR−/− piglets, while expression of TMEM16A was uncompromised. mRNA levels for TMEM16A, TMEM16F, and $\alpha\beta\gamma$ENaC were unchanged in CFTR−/− airways, while mRNA for SLC26A9 appeared reduced. CFTR was undetectable in epithelial cells of CFTR−/− airways and intestine. Small intestinal epithelium of CFTR−/− piglets showed mucus accumulation. Secretion of both electrolytes and mucus was activated by stimulation with prostaglandin E2 and ATP in the intestine of CFTR+/+, but not of CFTR−/− animals. pH was measured inside small bronchi using a pH microelectrode and revealed no difference between CFTR+/+ and CFTR−/− piglets. Intracellular pH in porcine airway epithelial cells revealed only a small contribution of CFTR to bicarbonate secretion, which was absent in cells from CFTR−/− piglets. In contrast to earlier reports, our data suggest a minor impact of CFTR on ASL pH. In contrast, enhanced amiloride-sensitive Na+ absorption may contribute to lung pathology in CFTR−/− piglets, along with a compromised CFTR- and TMEM16A-dependent Cl− transport.

Keywords CFTR · Chloride secretion · Bicarbonate transport · CFTR−/− piglets · Airways · Intestinal epithelium · Cystic fibrosis

Introduction

In contrast to mouse CFTR-knockout models for cystic fibrosis (CF) [13], the CF pig model accurately reproduces human CF lung pathology [8, 38]. Pezzulo et al. found that the airway surface liquid (ASL) pH was more acidic in CF pigs when compared with wild-type littermates. They further showed that lower pH in CF animals inhibited the antimicrobial

Roberta Benedetto and Raquel Centeio share first authorship

✉ Karl Kunzelmann
karl.kunzelmann@ur.de

1 Institut für Physiologie, Universität Regensburg, Universitätsstraße 31, D-93053 Regensburg, Germany

2 Institute of Molecular Animal Breeding and Biotechnology, Ludwig-Maximilians-Universität München, Munich, Germany

activity of ASL [40]. This correlated with impaired bacterial killing and disrupted mucociliary transport due to adhesive mucus, while enhanced airway Na+ absorption was not detected [18, 51]. Hoegger et al. demonstrated an abnormal mucociliary transport in CF airways even under submerged conditions, thus questioning the role of surface dehydration in CF lung disease [18]. A large number of additional studies demonstrated the role of Cl− and HCO$_3^-$ transport for proper mucociliary clearance [1, 9, 21, 24, 25]. A pathogenic concept was established in which CF lung disease starts with reduced HCO$_3^-$ secretion caused by impaired CFTR function. As a result, ASL acidification, impaired defense, inflammation, and mucus hypersecretion/adhesion attenuate mucociliary clearance and cause CF.

However, Schultz and coworkers assessed airway pH using an optical device connected to a fluorometer and measured pH directly in lungs of children with or without CF. They did not find evidence for acidic pH in the airways of CF children [47].

Moreover, Hug and Bridges did not find a change in intracellular pH of porcine submucosal gland cells upon cAMP-dependent stimulation of CFTR [19], and also Kim et al. reported an only limited contribution of CFTR to bicarbonate transport [27]. This is surprising given the reported impact of CFTR on ASL pH [40]. Due to these controversies, we aimed to analyze intrabronchial pH in piglets and intracellular pH in airway epithelial cells from CFTR+/+ and CFTR−/− piglets.

Chen et al. did not did detect an increase in transepithelial Na+ transport or enhanced liquid absorption in airways of CFTR−/− pigs, although an increase in amiloride-sensitive voltage was detected [8]. These results were in sharp contrast to the pathogenic concept of Na+ hyperabsorption in CF. According to this, enhanced electrolyte absorption driven by amiloride-sensitive Na+ absorption leads to airway dehydration and mucus plugging [6, 14, 33]. As a consequence, airway mucus plugging and impaired mucociliary clearance will lead to subsequent chronic bacterial infections. Because of these obvious contradictions, we re-examined ion transport in airways from CFTR+/+ and CFTR−/− piglets.

A CF pig model similar to the one described above was generated earlier by Klymiuk and coworkers [28]. CF-typical abnormalities were detected in the intestine, respiratory tract, and other epithelial organs, closely resembling human CF and the alterations observed in another CF pig model [36, 41]. Because functional parameters were not assessed in this CF pig model, we examined pH and ion transport in airways and the intestine. In contrast to [8, 40], we were unable to detect a lower pH in small airways. In contrast, we found evidence for enhanced Na+ absorption. The present data support the concept of airway dehydration and hyperabsorption as the primary cause for impaired mucus clearance in CF [17].

Methods

Generation of CFTR−/− piglets and tissue preparation Generation and breeding of CFTR+/+ and CFTR−/− littermate piglets were performed as described earlier [28]. In brief, CFTR−/− piglets have been generated by inactivating the CFTR gene in primary porcine cells by sequential targeting, using modified bacterial artificial chromosome vectors. The cells were then used to generate homozygous CFTR-mutant piglets by somatic cell nuclear transfer. All animal procedures were performed according to the German Animal Welfare Act with permission of the local regulatory authority of the LMU Munich. Piglets were euthanized within the first 24 h after birth under Ketamine (Ursotamin®, Serumwerk Bernburg, Germany) and Azaperone (Stresnil®, Elanco Animal Health, Bad Homburg, Germany) anesthesia by intracardiac injection of T61® (Intervet, Unterschleissheim, Germany).

Intrabronchial pH measurements Intrabronchial pH was assessed with a micro-pH electrode (Orion™ 9810BN, Thermo Scientific™, Schwerte, Germany). The electrode requires as little as 500 nl liquid to reliably determine pH values. Immediately after sacrificing the animals, lungs were removed, sliced and electrodes were placed 5 mm deep into cross-sectionally opened small airways with diameters between 1.5–3 mm. At least 10 pH readings were taken, and a mean value was determined for each airway. The spherical 1.3 mm pH electrode tip was polished and did not penetrate airway epithelial cells with a diameter of about 20 μM. The pH values obtained through these measurements represent the pH of airway surface liquid and mucus present in small airways.

Primary airway epithelial cell cultures Porcine bronchial epithelial (PBE) cells were harvested from isolated bronchi of wild-type (CFTR+/+) and CFTR-knockout (CFTR−/−) piglets as previously described for human lung cells [10]. In brief, primary cells were collected in bronchial epithelial cell basal medium supplemented with bovine pituitary extract, insulin, hydrocortisone, retinoic acid, transferrin, triiodothyronine, epinephrine, and human epidermal growth factor (Lonza, Basel, Switzerland). Cells were cultured using Rho kinase and dual SMAD signaling inhibition in the absence of a feeder-cell layer and were re-differentiated on permeable supports.

HE and Alcian blue staining, lipid peroxidation Histological analysis was performed as described earlier [2]. Tissues were fixed in 4% paraformaldehyde, picric acid, and sucrose in PBS and were washed in methanol before embedding in paraffin. Sections were stained with Alcian blue and assessed by light microscopy. A 4-HNE staining was used to analyze membrane lipid peroxidation, as described earlier [46]. Thirty images of 4 CFTR−/− animals and 6 images of 3 CFTR+/+ animals were examined. Sections were analyzed using an Axiovert200 microscope equipped with AxioCam ICc 1 and ApoTome (Zeiss, Oberkochen, Germany).

Immunocytochemistry Paraffin-embedded sections (5 μM) were blocked with 5% bovine serum albumin (BSA) and 0.04% Triton X-100 in PBS for 30 min. TMEM16A was detected using P79 anti-TMEM16A (1:300; Davids Biotechnology, Regensburg, Germany). CFTR was detected using mouse monoclonal anti-CFTR antibody #596, kindly provided by the North American CF foundation. The CFTR antibody was used at a dilution of 1:3000. Immunofluorescence was detected with an Axiovert 200 and analyzed using AxioVision software (AxioVs40; V 4.8.2.0; Zeiss, Jena, Germany).

RT-PCR For RT-PCR total RNA from lung tissue or porcine primary cells was isolated using NucleoSpin RNA II columns

(Macherey-Nagel, Düren, Germany). Total RNA (1 μg/50 μl reaction) was reverse-transcribed using random primer (Promega, Mannheim, Germany) and M-MLV Reverse Transcriptase, RNase H Minus (Promega, Mannheim, Germany). Semiquantitative RT-PCR was used to determine levels of expression for each transport protein. To that end, mRNA from at least $n = 3$ CFTR+/+ and $n = 3$ CFTR−/− animals was analyzed in a larger number of reactions. Each RT-PCR reaction contained sense and antisense primers (0.5 μM) (Table 1), 0.5 μl cDNA, and GoTaq Polymerase (Promega, Mannheim, Germany). After 2 min at 95 °C, cDNA was amplified (35 cycles for target sequence and 30 cycles for the reference GAPDH) for 30 s at 95 °C, 30 s at 56 °C, and 1 min at 72 °C. PCR products were visualized by loading on peqGREEN (Peqlab; Düsseldorf, Germany) containing agarose gels and analyzed using ImageJ.

In vitro perfusion of piglet jejunum ex vivo The methods for in vitro perfusion of excised intestinal section were explained in previous publications [2]. In brief, piglets were euthanized, and excised intestinal sections were placed immediately in ice-cold Ringer solution (mmol/l 145 NaCl, 0.4 KH2PO4, 1.6 K2HPO, 4.6 D-glucose, 1 MgCl2, 1.3 Ca²⁺ gluconate, pH 7.4). Sections were carefully flushed to remove residual luminal contents. Tissues were mounted into an Ussing chamber insert with a circular aperture of 0.785 mm². Luminal and basolateral sides of the epithelium were perfused continuously at a rate of 5 ml/min. Solutions were heated to 37 °C, using a water jacket. ENaC and cyclooxygenase were inhibited by amiloride (10 μM) and indomethacin (10 μM), respectively. IBMX (100 μM) and forskolin (2 μM) (IF) were used to measure CFTR-dependent Cl⁻ secretion in jejunal tissue. Carbachol (CCH; 100 μM) was used to activate Ca²⁺-dependent Cl⁻ transport. Experiments were carried out under open circuit conditions. Data were collected continuously using PowerLab (AD Instruments, Spechbach, Germany). Values for transepithelial voltages (V_{te}) were referred to the serosal side of the epithelium. Transepithelial resistances (R_{te}) were determined by applying short (1 s) current pulses ($\Delta I = 0.5$ μA). R_{te} and equivalent short circuit currents (Isc) were calculated according to Ohm's law ($R_{te} = \Delta V_{te}/\Delta I$, Isc $= V_{te}/R_{te}$). To assess mucus secretion, intestinal segments were mounted and perfused basolaterally in a custom-designed perfusion chamber, with HCO_3^- containing Ringer solution at 37 °C and bubbling with 95% O_2/5% CO_2, as described earlier (Fig. 3e) [2]. The lumen was perfused with glucose-free, HCO_3^- Ringer solution at a rate of approximately 0.5 ml/min. The system was let run for 30 min to remove residual luminal contents. Mucus release was stimulated by apical PGE_2 and ATP. Apical perfusates were collected in 3-min intervals, and DTT was added to dissolve mucus. Mucin content of the luminal perfusates was analyzed using Periodic acid-Schiff (PAS) and absorbance assays. Values were normalized to the weight of the jejunal section.

Intracellular pH measurements Porcine primary cells were incubated in Ringer solution (mmol/l NaCl 118.75; KH2PO4 0.4; K2HPO4 1.6; glucose 5; MgCl2 1; Ca-gluconate 1.3; probenecid 2.5; Na-gluconate 25) containing 2 μM BCECF-AM (Life Technologies GmbH, Darmstadt, Germany) and 0.02% Pluronic (Life Technologies) for 60 min at 20 °C. For intracellular pH measurements, cells were mounted in a cell chamber and perfused at 37 °C with HCO_3^-/CO_2 containing Ringer solution (mmol/l, NaCl 118.75; KH2PO4 0.4; K2HPO4 1.6; glucose 5; MgSO4 1; Ca-gluconate 1.3; probenecid 2.5; NaHCO3 25; bubbled with

Table 1 Primers for RT-PCR

CFTR	Forward: 5′- AACCTGAACAAGTTTGATGAAG	480 bp
	Reverse: 5′- CAGAACAATGCAGAATGAGATG	
TMEM16A	Forward: 5′- CGTCATCATCAACCTGGTGG	587 bp
	Reverse: 5′- CCAGGCGGATCTCAATGATG	
TMEM16F	Forward: 5′- GGAGTTTTGGAAGAGGCGC	579 bp
	Reverse: 5′- CAATAAACTGGATCTCCTGGG	
SLC26A4	Forward: 5′- CACCATCGACGGGAATCAG	672 bp
	Reverse: 5′- GCAAGTAAACACCCAGATAAC	
SLC26A9	Forward: 5′- CATACTCCCTCACCCTCTTC	433 bp
	Reverse: 5′- CTCTCATTGGTGGCATTGTTG	
SCNN1A	Forward: 5′- CTGCAACAACACCACCATCC	313 bp
	Reverse: 5′- GGAGTTGTACTTGTACAGGTC	
SCNN1B	Forward: 5′- GTGACAACACCAACACCCAC	598 bp
	Reverse: 5′- GAGAAGATGTTGGTGGCCTG	
SCNN1G	Forward: 5′- GCGCCCACTATCAAGGAGC	454 bp
	Reverse: 5′- CCTTGCCCGTCTCACCTTG	
GAPDH	Forward: 5′- CATCGGGCGCCTGGTCAC	199 bp
	Reverse: 5′- CTCCTGGAAGATGGTGATGG	

95% O_2/5% CO_2). Pendrin activity was measured by the initial slope of pH increase after applying Cl^--free HCO_3^-/CO_2 solution (Na-gluconate 118.75; KH2PO4 0.4; K2HPO4 1.6; glucose 5; MgSO4 1; Ca-gluconate 1.3; probenecid 2.5; NaHCO3 25; bubbled with 95% O_2/5% CO_2) and Cl^--free iodide solution (Na-gluconate 118.75; KH2PO4 0.4; K2HPO4 1.6; glucose 5; MgSO4 1; Ca-gluconate 1.3; probenecid 2.5; NaHCO3 25; bubbled with 95% O_2/5% CO_2). For pH calibration, cells were perfused with buffers of variable pHs between 6.5 and 8.5 containing 105 mosmol/l KCl, 1 mmol/l MgCl2, 30 mmol/l HEPES, and 5 μmol/l nigericin. Excitation wavelengths of 440 and 490 nm were used, and emission intensity at 535 nm was recorded using a high speed polychromator system and a CoolSnap HQ camera (Visitron Systems, Puchheim, Germany). Control of experiment, imaging acquisition, and data analysis were done with the software package Meta-Fluor (Universal imaging, USA).

Patch clamping Cells were grown on coated glass coverslips for patch clamp experiments. Patch pipettes were filled with a cytosolic-like solution containing in mM, KCl 30; K-gluconate 95; NaH_2PO_4 1.2; Na_2HPO_4 4.8; EGTA 1; Ca-gluconate 0.758; $MgCl_2$ 1.03; D-glucose 5; ATP 3; and pH 7.2. The Ca^{2+} activity was 0.1 μM. Coverslips were mounted in a perfused bath chamber on the stage of an inverted microscope (IM35, Zeiss) and kept at 37 °C. The bath was perfused continuously with Ringer solution at a rate of 8 ml/min. Patch clamp experiments were performed in the whole cell configuration. Patch pipettes had an input resistance of 4–6 MΩ when filled with cytosolic like solution. Currents were corrected for serial resistance. The access conductance was monitored continuously and was 60–140 nS. Currents (voltage clamp) and voltages (current clamp) were recorded using a patch clamp amplifier (EPC 7, List Medical Electronics, Darmstadt, Germany), the LIH1600 interface and

Fig. 1 Structural changes in airways from CFTR−/− piglets. **a** Comparison of cross-sections of tracheas from CFTR+/+ ($n = 2$) and CFTR−/− ($n = 2$) newborn piglets. Bars = 500 μM. **b** Higher magnification showing defective cartilage structure in muscle bundles in CFTR−/− tracheas. Bars = 80 μM. **c** Small airways from CFTR+/+ ($n = 3$) and CFTR−/− ($n = 3$) newborn piglets. Dark precipitation is caused by 4-hydroxy-2-nonenal (4-HNE) staining, indicating membrane lipid peroxidation of airway epithelial cells in CFTR−/− tracheas. Typically, 34–40 images were examined in each series. Bars = 50 μM
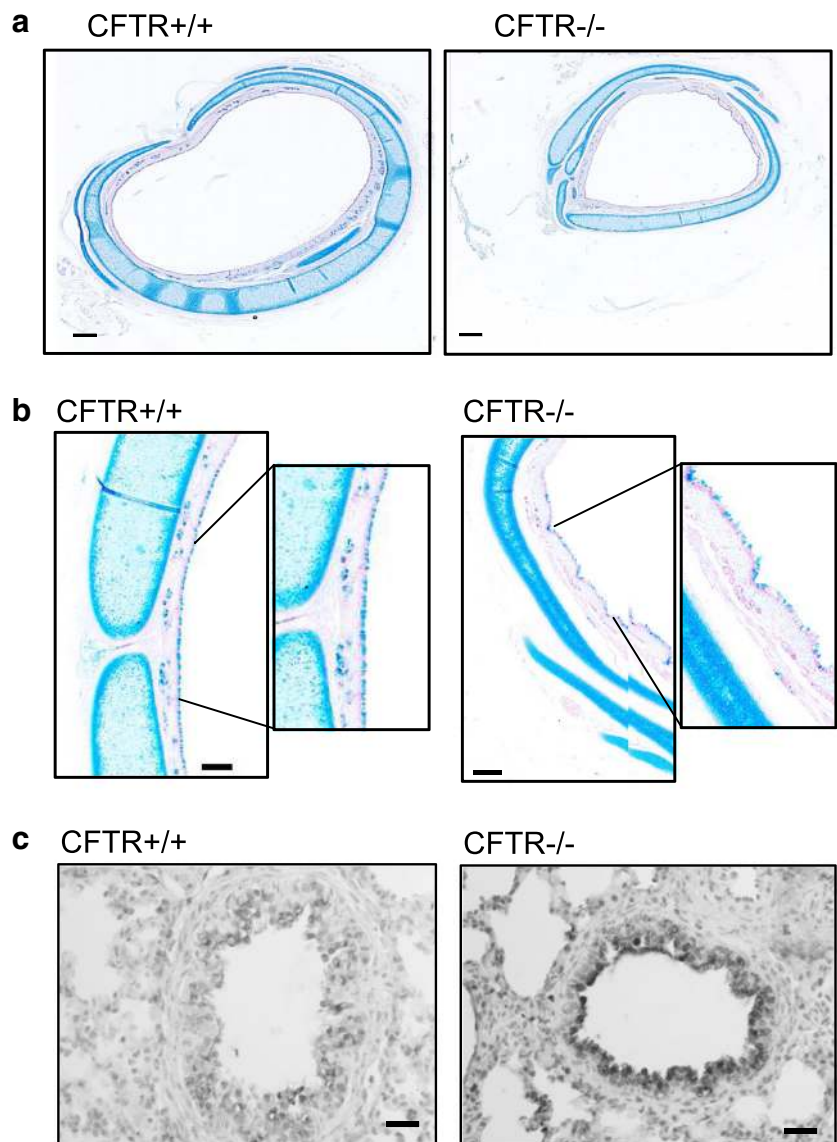
PULSE software (HEKA, Lambrecht, Germany), as well as the Chart software (AD Instruments, Spechbach, Germany). Data were stored continuously on a computer hard disc and analyzed using PULSE software. At regular intervals, the membrane voltage (Vc) was clamped in steps of 20 mV from − 100 to + 100 mV from a holding voltage of − 100 mV.

Transepithelial Ussing chamber recordings Filter-grown airway epithelial cells were measured under open or short circuit conditions as detailed in previous reports [4, 29]. In brief, PBE cells were grown on Millipore filters in an air-liquid interface (ALI) in Advanced DMEM/F12 media (Thermo Fisher Scientific, USA) supplemented with 0.5 µg/mL hydrocortisone, 100 nM triiodothyronine, and 0.5 µg/mL epinephrine (all from Sigma-Aldrich, Missouri, USA); 0.25 µg/mL human epidermal growth factor (PeproTech, UK); 100 nM TTNPB

(Cayman, USA); and 50 nM A83-01 (Tocris Bioscience, Bristol, UK) for 14–21 days. For the first week of ALI, 500 nM A83-01 was supplemented, and for the second week, 10 µM of DAPT (Tocris Bioscience, Bristol, UK) was added.

Materials and statistical analysis All compounds used were of highest available grade of purity. Data are reported as mean ± SEM. The data were symmetrically distributed as continuous (not ordinal) data. Student's t test (for paired or unpaired samples as appropriate) and ANOVA were used for statistical analysis. A p value < 0.05 was accepted as significant difference. The total number of CFTR+/+ and CFTR−/− animals was 13 and 14, respectively. For each experimental series, the number of animals used and the number of measurements/assays/reactions are provided (number of animals/number of experiments).

Fig. 2 Expression of ion channels in porcine airway epithelial cells. a Expression of CFTR and TMEM16A (green fluorescence) in airways from newborn CFTR+/+ and CFTR−/− piglets. In WT lungs, CFTR is expressed predominately in submucosal glands (SG). Some expression is found in the surface epithelium (SE). No expression of CFTR is detected in CFTR−/− lungs. In CFTR+/+, TMEM16A is expressed in SE and SG at low level but appears somewhat upregulated in lungs of CFTR−/− animals. Cilia (acetylated tubulin, red) and nuclei (DAPI). About 20–25 images of each $n = 3$ CFTR−/− and CFTR+/+ animals were examined. b Analysis of mRNA expression for TMEM16A, TMEM16F, CFTR, SLC26A9, and αβγENaC (SCNN1A, SCNN1B, SCNN1G) in airway epithelial cells from newborn CFTR+/+ and CFTR−/− piglets. Mean ± SEM (number of animals/number of reactions). #Significant difference when compared to CFTR+/+ ($p < 0.05$, unpaired t-test)
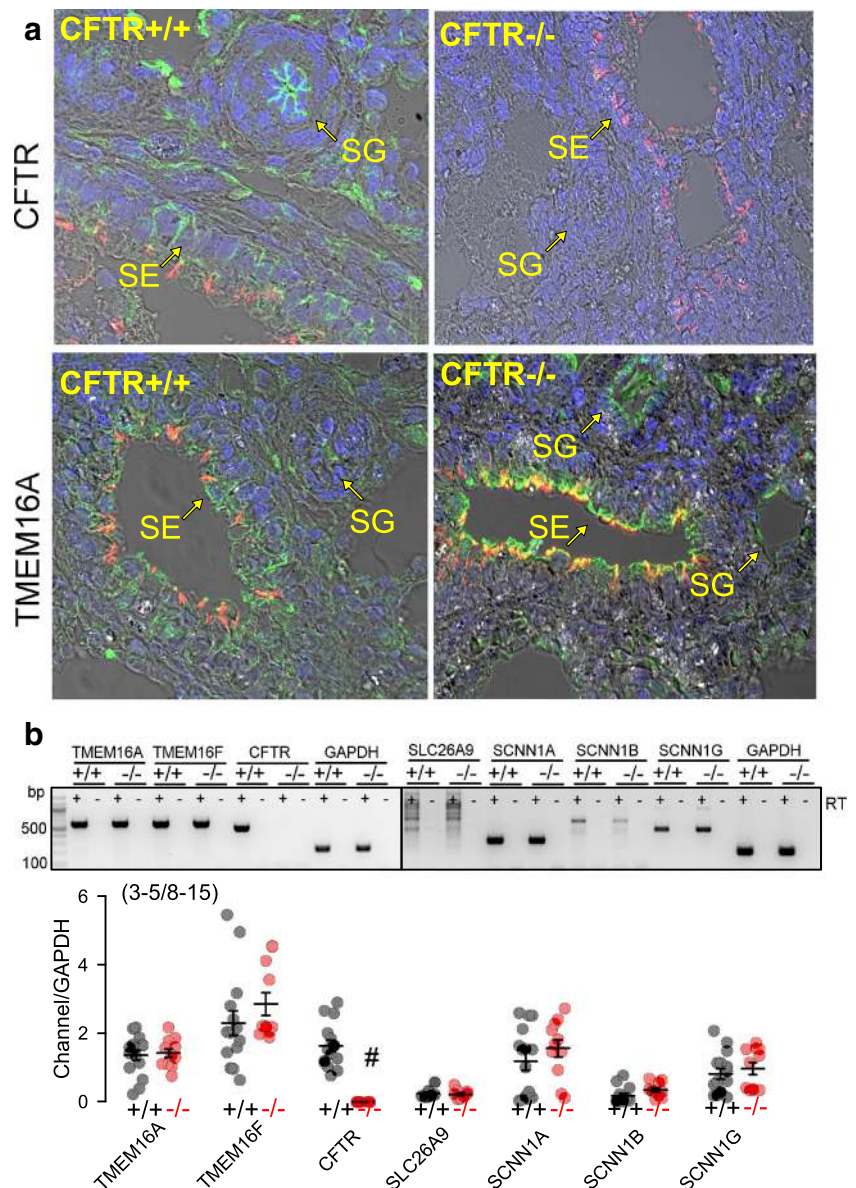
Results

Airway abnormalities in newborn CFTR−/− piglets Generation and basic pathological properties of CFTR−/− piglets have been described in a previous report [28]. Due to local ethical regulations and 100% penetrance of the meconium ileus, piglets needed to be sacrificed 24 h after birth. Discontinued tracheal cartilage rings and altered orientation of smooth muscle cell bundles described by Klymiuk et al. [28] were also observed in the present study (Fig. 1a,b). Similar to the CFTR −/− piglets described by Rogers et al. [41], we also did not observe accumulation of mucus in small or larger airways of CFTR−/− piglets, and no evidence was found for mucus plugging. Rogers et al. did not detect evidence for airway/lung inflammation in newborn CFTR−/− piglets, arguing against early lung inflammation in young infants before bacterial colonization [41]. We examined whether lipid peroxidation as an early inflammatory marker is present in small airways of newborn CFTR−/− piglets. This would provide hints as to an early lung inflammation in CF. Notably, in 3 out of 4 piglets examined, evidence for lipid peroxidation of airway epithelial cells was detected using 4-HNE staining, while none of the CFTR+/+ piglets showed significant staining (Fig. 1c).

Expression of CFTR and TMEM16A We examined the expression of CFTR and the Ca^{2+}-activated Cl^- channel TMEM16A using immunohistochemistry. In CFTR+/+ airways, CFTR was well expressed in airway submucosal glands and surface epithelium, while no CFTR was detected in CFTR−/− animals (Fig. 2a). TMEM16A was found in submucosal glands and surface epithelium of CFTR+/+ piglets and was also present in airways of CFTR−/− animals. mRNA expression for TMEM16A, TMEM16F, SLC26A9, and $\alpha\beta\gamma$ENaC were found to be similar in CFTR+/+ and CFTR−/− airway

Fig. 3 Lack of intestinal fluid and mucus transport in CFTR−/− piglets. **a** Histology and Alcian blue staining of intestinal epithelium from CFTR+/+ and CFTR−/− piglets. Bars = 100 μM. Representative stainings from $n = 2$ CFTR+/+ and CFTR −/−, respectively, with 22–23 images being analyzed. **b** Expression of TMEM16A, TMEM16F, and CFTR in intestinal epithelial cells from CFTR+/+ and CFTR−/− piglets as detected by RT-PCR. **c** Original Ussing chamber recordings of transepithelial voltages (open circuit) from freshly isolated jejunal epithelium obtained from CFTR+/+ (upper recoding; black) and CFTR−/− (lower recording; red) piglets. **d** Comparison of calculated short circuit currents activated by basolateral IBMX (100 μM) and forskolin (2 μM) (IF) or the muscarinic agonist carbachol (CCH, 100 μM). **e** Scheme for the perfusion of isolated CFTR+/+ and CFTR−/− jejunum ex vivo (left) and **f** time course for mucus release induced by luminal perfusion with PGE_2 (1 μM) and ATP (100 μM). Mean ± SEM (number of animals/ number of experiments or reactions). #Significant difference when compared with CFTR+/+ ($p < 0.05$, ANOVA)
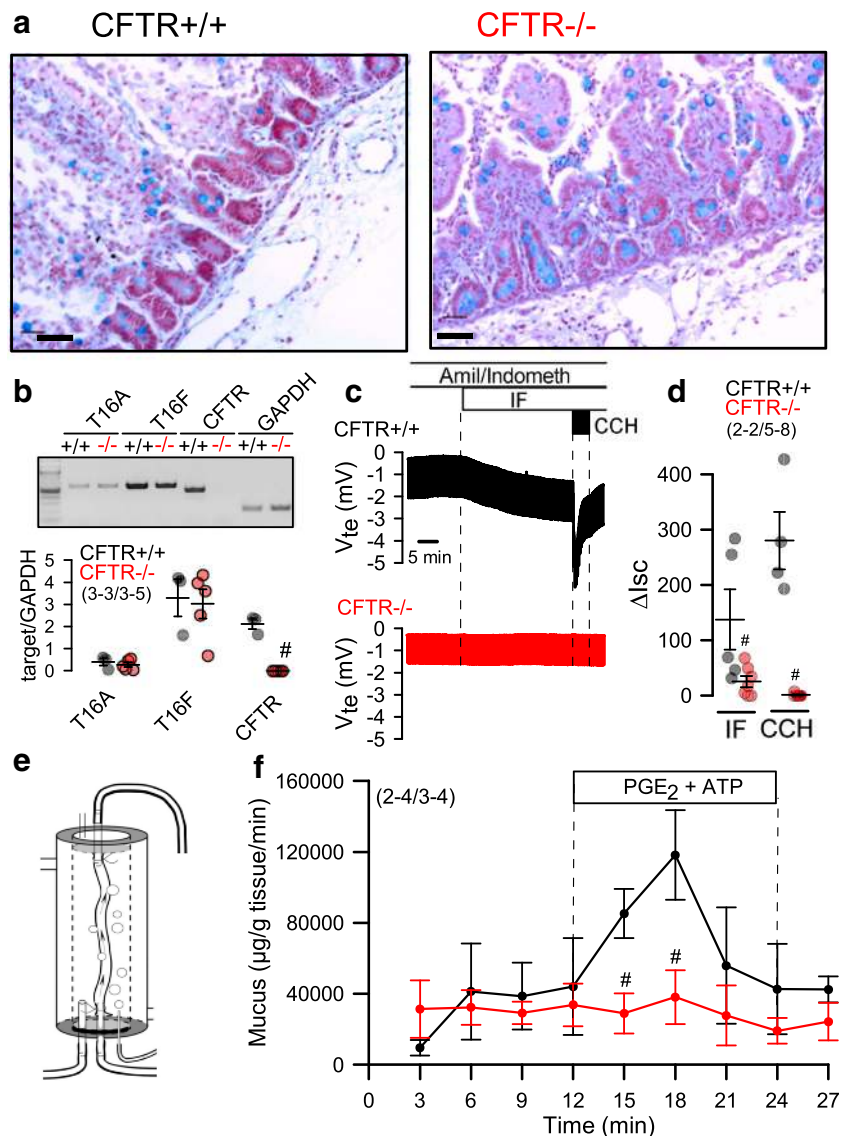
epithelial cells, while CFTR-mRNA was completely absent in CFTR−/− (Fig. 2b).

Lack of intestinal chloride and mucus secretion in CFTR−/− piglets Klymiuk et al. described an intestinal phenotype in CFTR−/− piglets, resembling the severe intestinal phenotype observed in CF [28]. A similar phenotype was found in another CFTR−/− model described earlier [41]. In the present study, mucus accumulation was present in small intestinal crypts of CFTR−/− animals (Fig. 3a). Expression of CFTR-mRNA was absent in isolated crypt epithelial cells from CFTR−/− animals, while expression of TMEM16A or TMEM16F-mRNA was similar to that in CFTR+/+ animals (Fig. 3b). In Ussing chamber recordings of small intestinal sections of CFTR−/− piglets, we observed a complete absence of both cAMP-activated (IF) and Ca^{2+}-activated (CCH) Cl^- transport (Fig. 3c,d). This result confirms earlier findings obtained in human intestinal biopsies, showing that Ca^{2+}-dependent electrolyte secretion relies entirely on the presence of apical CFTR [34]. We reported earlier mouse intestinal mucus

secretion by apical purinergic stimulation [2]. Using the same method of in vitro perfused intestinal loops (Fig. 3e), we found that ATP and PGE_2-induced mucus secretion was completely absent in small intestine freshly removed from CFTR−/− animals (Fig. 3f). The results are in line with earlier findings in mouse, demonstrating the essential role of CFTR for intestinal mucus secretion [48].

CFTR−/− piglets do not exhibit low bronchiolar pH Evidence has been presented for reduced tracheal surface pH in CF pigs [40]. In the present CF porcine model, we assessed intrabronchial pH using a micro-pH electrode. The electrode had a very small tip diameter allowing pH measurements directly in small airways. pH was assessed in peripheral airways of different sections in each lung. We detected a mean value for pH value of about 7.1 in airways of CFTR+/+ piglets, which corresponded well to the pH value detected in vivo in CFTR+/+ piglets reported by Pezzulo and coworkers [40]. However, in contrast to this study, we did not detect a lower pH value in airways of CFTR−/− piglets (Fig. 4a).

Fig. 4 Limited impact of CFTR on pH regulation in piglet airways. **a** Intraluminal pH measured in bronchioles of CFTR+/+ and CFTR−/− piglets. Per animal, $n = 7$–24 measurements were taken and pooled. **b,c** Intracellular pH (pH_i) measured in airway epithelial cells isolated from newborn CFTR+/+ and CFTR−/− piglets. Stimulation with IF had little but significant effects on pH_i of CFTR+/+ cells. **d,e** Original recordings of pH_i in airway epithelial cells from CFTR+/+ and CFTR−/− piglets. Effect of removal of extracellular Cl^- (0 Cl^-) and addition of I^- (0 Cl^-/I^-) on pH_i in the absence or presence of IF. **f** Summaries of the experiments shown in (**d,e**). $n = 3$ CFTR+/+ and CFTR−/− animals. Per animal, $n = 10$–69 measurements were taken and pooled. **g,h** Expression of CFTR and SLC26A4 in airway epithelial cells from CFTR+/+ and CFTR −/− piglets as detected by RT-PCR. Mean ± SEM (number of animals/number of measurements). *Significant effect of IF and 0 Cl^-, respectively. #significant difference when compared with CFTR+/+, respectively ($p < 0.05$, ANOVA)
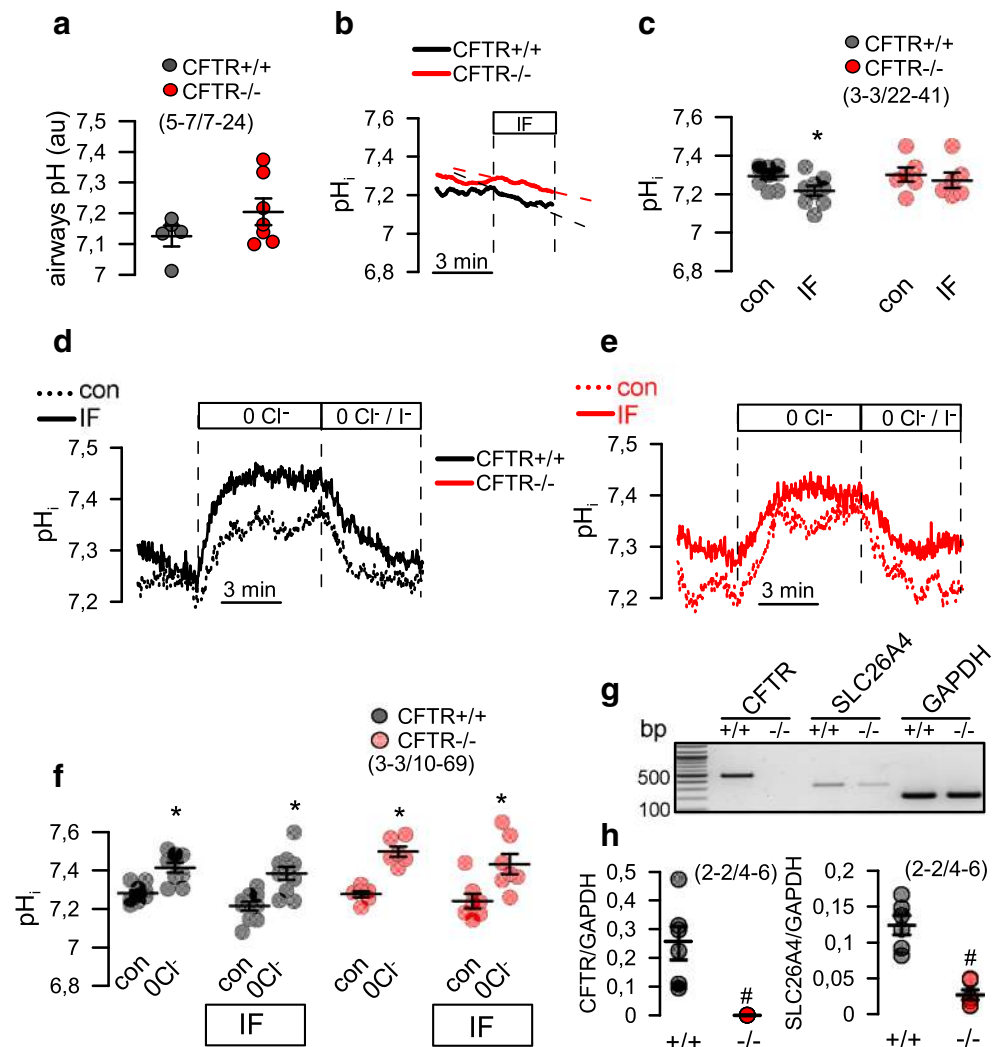
Limited contribution of CFTR to regulation of intracellular pH

This result prompted us to measure intracellular pH in primary bronchial airway epithelial cells. We found that intracellular pH was similar in cells from CFTR+/+ and CFTR−/− piglets and was between 7.2 and 7.3. pH was only slightly acidified upon stimulation with IF in CFTR+/+ but not in CFTR−/− cells, suggesting an only limited contribution of CFTR to bicarbonate secretion (Fig. 4b,c). Removal of extracellular Cl⁻ caused an intracellular alkalization in both CFTR+/+ and CFTR−/− cells, while IF did not further increase intracellular alkalization (Fig. 4d–f). Moreover, we found expression of pendrin mRNA being lower in CFTR−/−, when compared with CFTR+/+ cells (Fig. 4g,h). Taken together, the data suggest a limited contribution of CFTR to the regulation of intracellular pH in porcine airway epithelial cells. As reported

earlier, other transport proteins, such as pendrin, might be more important for pH regulation in airway epithelial cells [11, 15].

Enhanced Na⁺ absorption and defective cAMP and Ca²⁺-dependent Cl⁻ secretion in CFTR−/− airway epithelial cells Cl⁻ and Na⁺ transport was analyzed in the absence of bicarbonate in polarized grown airway epithelial cells from CFTR+/+ and CFTR−/− piglets. We first used open circuit conditions in a perfused micro-Ussing chamber, to analyze transepithelial voltages (V_{te}). We found slightly but significantly augmented V_{te} in CFTR−/− monolayers and enhanced inhibition of V_{te} by amiloride ($\Delta V_{te\text{-Amil}}$). The calculated equivalent short circuit currents inhibited by apical amiloride ($\Delta I_{sc\text{-Amil}}$) was enhanced in CFTR−/− epithelia (Fig. 5a,b). The data may indicate

Fig. 5 Comparison of ion transport in airway epithelial cells from CFTR+/+ and CFTR−/− piglets. **a** Open circuit Ussing chamber measurements on polarized grown airway epithelial cells from CFTR+/+ and CFTR−/− piglets in the absence of CO_2/HCO_3^-. Effects of amiloride (10 μM). **b** Comparison of voltage deflections and calculated equivalent short currents (Isc). **c,d** Effect of IBMX/forskolin (IF 100/2 μM) and CFTRinh172 (30 μM) on transepithelial voltages and Isc. **e,f** Effect of IF and bumetanide (100 μM) on transepithelial voltages and Isc. **g,h** Effect of luminal ATP (100 μM) on transepithelial voltages and Isc (pk, peak current; pl, plateau current). **i,j** Effect of luminal ATP (100 μM) in the presence of niflumic acid (NFA; 10 μM) on transepithelial voltages and Isc. Mean ± SEM (number of animals/number of measurements). *Significant effects of IF, Bum, or ATP ($p <$ 0.05, paired t-test). #Significant difference when compared with CFTR+/+ ($p < 0.05$, unpaired t-test). $Significant difference when compared with the absence of NFA ($p < 0.05$, unpaired t-test)
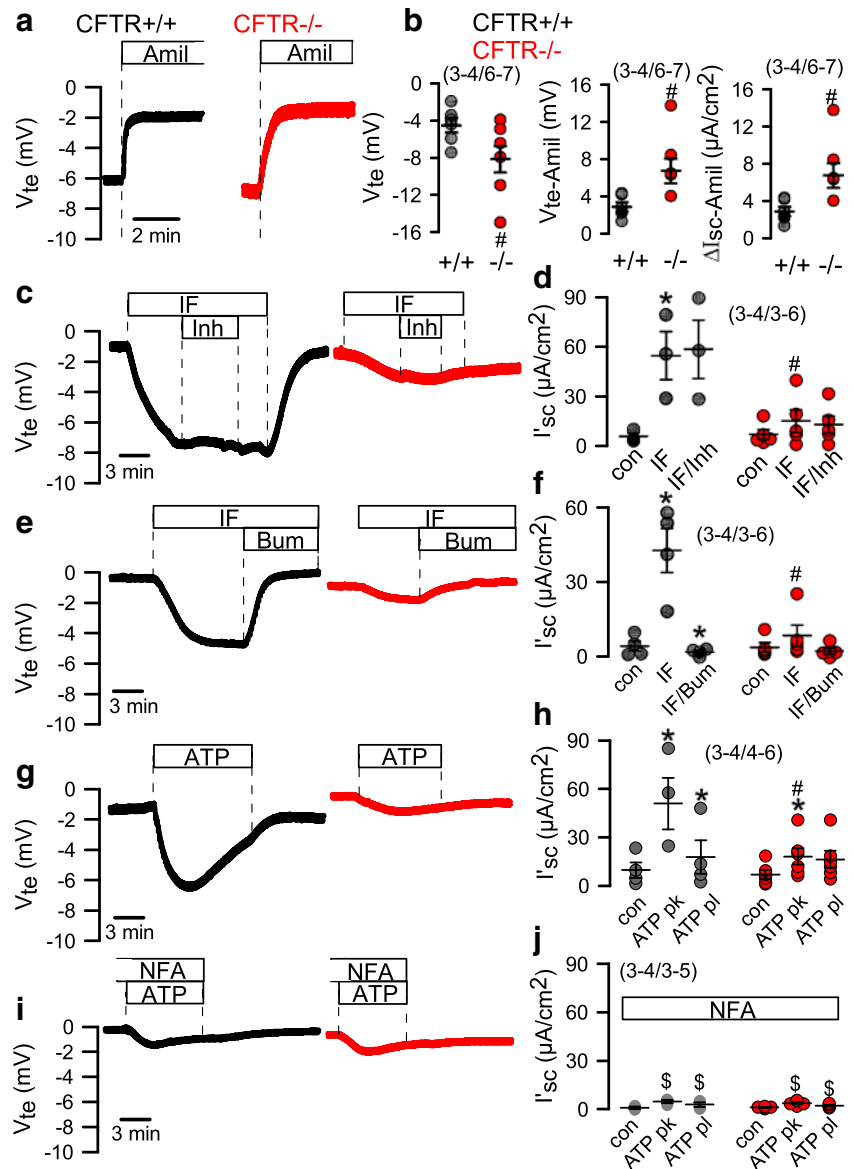
enhanced Na$^+$ absorption in CF airways. In contrast, lumen negative voltage deflections induced by cAMP-dependent stimulation (IF) were largely reduced in CFTR−/− cells, indicating a lack of CFTR expression (Fig. 5c). Surprisingly, luminal application of the CFTR inhibitor CFTRinh172 did not inhibit IF-induced Cl$^-$ secretion in CFTR+/+ airways. However, this has also been observed earlier in naïve tissues or mucus producing monolayers. In contrast, the NKCC1 inhibitor bumetanide (Bum, basolateral) completely abolished Cl$^-$ transport in CFTR+/+ monolayers and also blocked the small transport observed in CFTR−/− cells (Fig. 5c–f).

Notably, Ca^{2+}-dependent Cl$^-$ secretion induced by luminal ATP demonstrated a similar kinetic as IF-induced secretion and was also inhibited in CFTR−/− cells (Fig. 5g,h). ATP-activated secretion in CFTR+/+ cells was fully inhibited by the TMEM16A blocker niflumic acid. These results and previous reports suggest that receptor-mediated Ca^{2+}-activated Cl$^-$ secretion in porcine and human airways essentially occurs through CFTR, which, however, requires the function of TMEM16A [5, 37]. Although still incompletely understood, expression and/or function of TMEM16A appears essential to transmit signals from P2Y$_2$ - receptors to CFTR [4, 31].

In contrast to an earlier report, the present data suggest enhanced Na$^+$ absorption in airways of CFTR−/− piglets [8]. We performed additional transepithelial measurements under real short circuit conditions and in the presence of HCO$_3^-$ (Fig. 6a). Short circuit currents were strongly inhibited by amiloride and were larger in monolayers from CFTR−/− piglets (Fig. 6a,b). In the presence of amiloride, IF-induced Isc was significantly reduced in CFTR−/− monolayers but was still well detectable (Fig. 6c,d). Bumetanide inhibited the short circuit current in CFTR+/+, but not CFTR−/− monolayers. The remaining portion of IF-activated Isc was blocked by S0859, an inhibitor of the basolateral sodium bicarbonate cotransporter (NBC) (Fig. 6c,d). Taken together, the data suggest an upregulated Na$^+$ absorption by the epithelial Na$^+$ channel ENaC, a lack of cAMP-activated Cl$^-$ secretion in CFTR−/− cells, and a significant cAMP-activated HCO$_3^-$ transport that is reduced but still detectable in CFTR−/− airways.

Ion transport was also assessed in patch clamp experiments
Here, we found activation of CFTR whole cell currents by stimulation with IF in CFTR+/+ cells. IF-activated currents were inhibited by CFTRinh172 (Fig. 7a). In contrast, no currents were activated by IF in CFTR−/− cells. Ca^{2+}-activated whole cell currents were activated by ATP and were found to be reduced in CFTR−/− cells (Fig. 7b). Thus, both cAMP-dependent and Ca^{2+}−activated secretions are compromised in the airways of CFTR-knockout piglets. Moreover, in contrast to polarized grown epithelial cells and naive airways, the strict CFTR-dependence of ATP-activated Cl- currents is lost in non-polarized cells. We conclude that the direct Cl-transporting capacity of TMEM16A in piglet and human airways is probably negligible.

Fig. 6 Cl$^-$ and HCO$_3^-$ transport in airway epithelial cells from CFTR+/+ and CFTR−/− piglets. **a,b** Short circuit Ussing chamber measurements on polarized grown airway epithelial cells from CFTR+/+ and CFTR−/− piglets in the presence of 5% CO$_2$ and 25 mM HCO$_3^-$. Pronounced inhibition of Isc by amiloride (10 μM). **c** Summaries for the activation and inhibition of Isc by subsequent addition of IF, Bum, and S0859 (S, 30 μM). Mean ± SEM (number of animals/number of filters). *Significant effects of IF, Bum, or S ($p < 0.05$, paired t-test). Difference when compared with the absence of IF or when compared with CFTR+/+. #Significant difference when compared to CFTR+/+ ($p < 0.05$, unpaired t-test).^

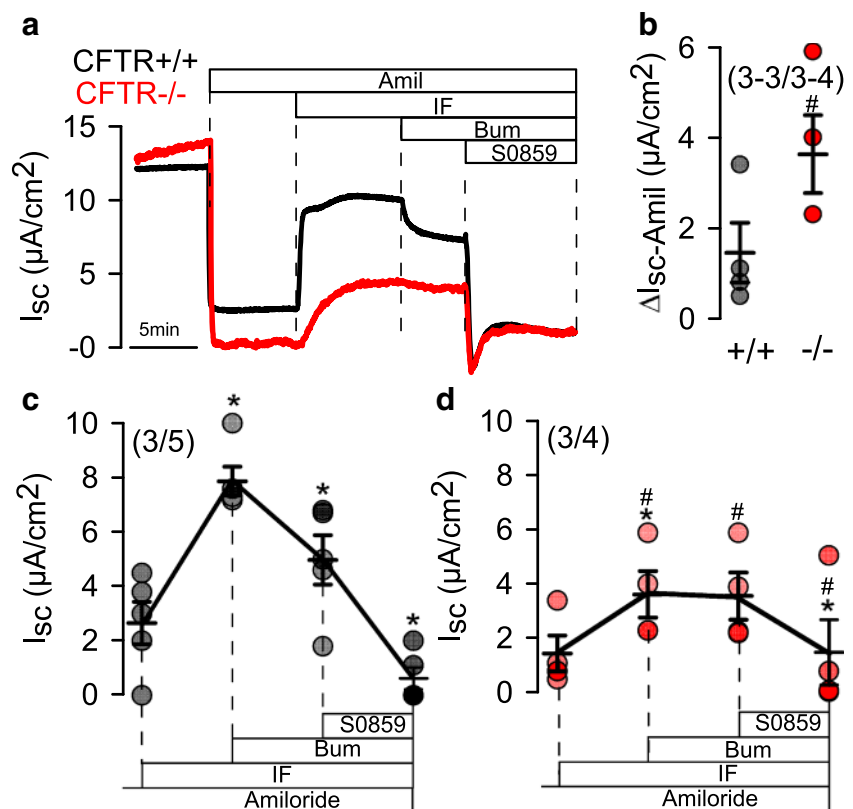**Fig. 7** Ion currents in airway epithelial cells from CFTR+/+ and CFTR−/− piglets. **a,b** Ion current overlays and current/ voltage relationships obtained in whole cell patch clamp recordings with airway epithelial cells from CFTR+/+ and CFTR−/− piglets. **a** IBMX/forskolin (IF, 100/2 μM) activated whole cell currents were only detected in cells from CFTR+/+ animals. Currents were inhibited by 30 μM CFTRinh172 (CFinh). **b** ATP (100 μM) activated whole cells were reduced in CFTR−/− cells. Mean ± SEM (number of animals/number of cells). *Significant effects of IF, ATP, or CFinh ($p < 0.05$, paired t-test). #Significant difference when compared with CFTR+/+ ($p < 0.05$, unpaired t-test)
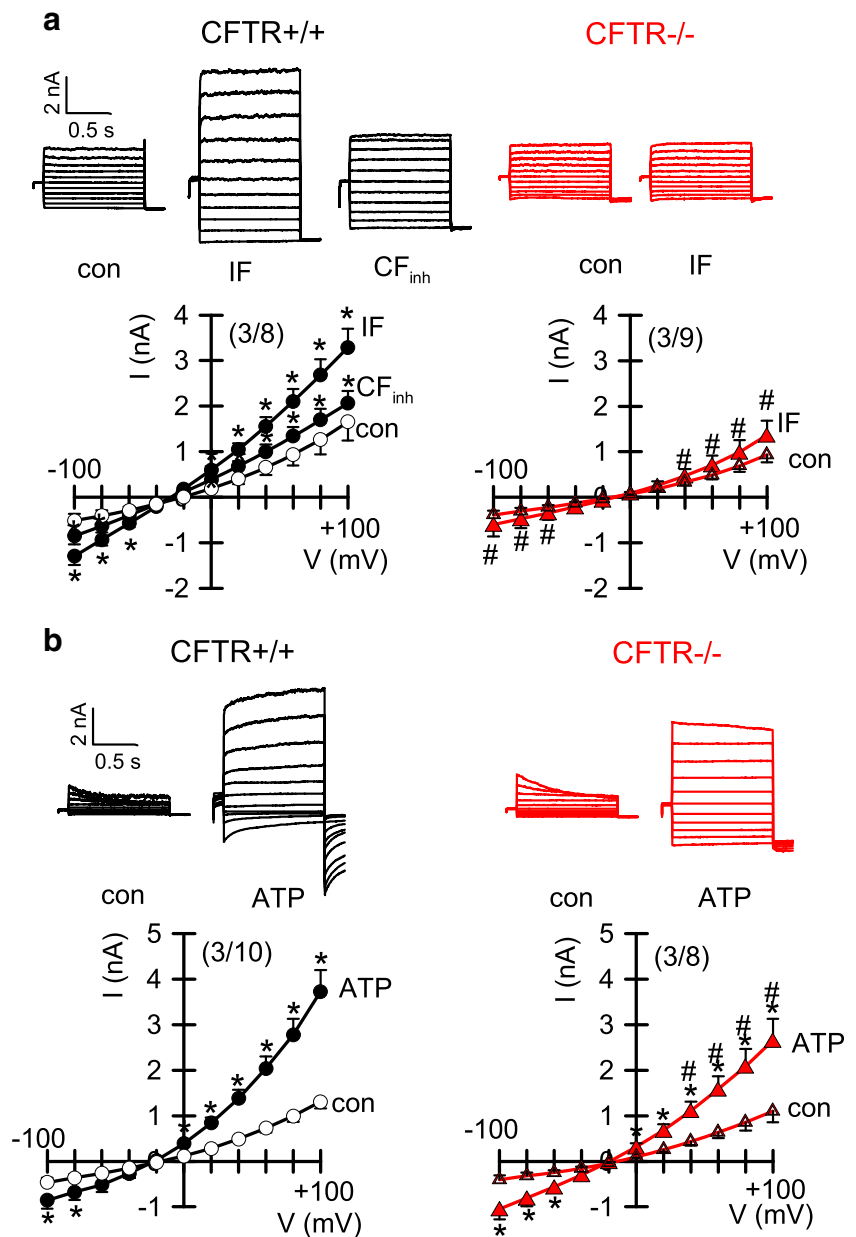
Discussion

The present data compare functional aspects of airway and intestinal epithelial cells from newborn WT and CFTR-knockout piglets [28]. Pulmonary oxidative stress response and abnormal bioactive lipids have been demonstrated in CF lung disease [20, 45], suggesting early pulmonary inflammation [42, 52]. Lipid peroxidation was also detected in the present study in the airways of newborn CFTR−/− piglets, providing evidence for an early pulmonary inflammation in the absence of bacterial colonization (Fig. 1). CF epithelial cells were shown earlier to have a compromised anti-oxidant defense by superoxide dismutase [43]. Finally, some CFTR-knockout mouse models did show signs of lung/airway

inflammation even in the absence of mucus obstruction [53]. Thus, early intrinsic inflammation without mucus plugging or bacterial infection may initiate CF lung disease [45].

While intrabronchial mucus accumulation or mucus plugging was not observed in airways of newborn CF piglets, accumulation of mucus in small intestinal crypts was obvious and comparable to earlier observations [28, 41]. In vitro perfusion of the small intestine from CFTR−/− piglets with luminal ATP could not induce mucus release (Fig. 3). In contrast, stimulation of CFTR+/+ jejunum by luminal ATP induced mucus secretion similar to mouse small and large intestine [2]. Notably, stimulation by prostaglandin E2 or ATP alone did not induce mucus secretion [2, 7]. These data correspond very well to the goblet cell dysfunction detected earlier in CF

intestine, which is likely to contribute to intestinal obstruction and inflammation in CF [32].

In contrast to a previous report on another porcine CFTR-knockout model [40], we did not find evidence for a reduced pH in small airways of CFTR−/− piglets (Fig. 4). Correspondingly, we found no difference in intracellular pH of CF and non-CF porcine airway epithelial cells under resting conditions and little impact of CFTR on intracellular pH. Bicarbonate transport was reduced in CF airway epithelia but nevertheless was still detectable (Fig. 6c,d). These data along with previous studies suggest that pendrin-dependent HCO_3^- secretion may be more important in controlling ASL pH [11, 27, 50]. We are confident that our intrabronchial microelectrode measurements were correct, as the standard curve obtained with this electrode provided reliable and reproducible pH readings (Fig. 8). Moreover, control measurements of mouse intratracheal pH showed a value of 6.98 ± 0.16 ($n = 33$), which corresponded well with other intratracheal in vivo measurements described earlier [23, 49]. Moreover, intraluminal measurements in mouse intestine showed pH values of 3.4 for stomach and 6.5 for colon, which is similar to earlier results [35]. Therefore, the pH values obtained in piglet airways probably reflect the true situation. For comparison, we also measured intratracheal pH in mice with an airway-selective knockout of TMEM16A (T16A$^{flox/flox}$-FoxJ1Cre) [4]. Notably, the intratracheal pH in these animals was significantly lower when compared with WT animals (Fig. 8b). Thus, TMEM16A is likely to contribute to the regulation of ASL pH. In fact, TMEM16A was shown earlier to be permeable for bicarbonate and has been discussed as a potential channel for bicarbonate release in the airway epithelium [12, 16, 26]. Despite the evidence for acidic airways in T16A$^{flox/flox}$-FoxJ1Cre mice, the animals did not show any lung pathology [4], again questioning the role of acidic pH for lung pathology in CF.

Pezzulo et al. reported lower pH values of the airway surface liquid (ASL) covering the tracheal epithelium of newborn CFTR−/− piglets. It is possible that the pH of tracheal and bronchial ASL may be different. However, regarding the CF lung disease, intrabronchial pH values are probably more relevant to the disease. Saint-Criq et al. performed long-term ASL pH measurements on fully differentiated primary human airway epithelial cells under very stable conditions [44]. ASL pH was found not to be different between non-CF and CF under resting (non-stimulated) conditions, but was enhanced in non-CF after stimulation with forskolin. Schulz and collaborators measured ASL pH in vivo in children using a luminescence technology integrated with fiber optic probes. They demonstrated that ASL pH in children with CF is similar to that of children without CF [47]. Our pH measurements directly in the lumen of small bronchi support these findings, as they revealed similar pH values in CF and non-CF piglets.

Because ASL thickness is just a few microns, accurate pH assessments are difficult. Probably any pH measurement technique has its own drawbacks, whether it is done by pH sensitive foils (CO_2 alterations), optical pH probes (light scattering by mucoid environment), in vitro measurements (incomplete differentiation, lack of submucosal glands), or pH electrode measurements (accurate location of electrodes). In addition, anesthesia compromises breathing patterns and circulation, while immediate measurement postmortem affects ion transport and CO_2. More work is required to solidify the concept of airway acidification as the cause for defective host defense in CF [49, 50]. At any rate, the pathogenic concept of airway acidification as the initiator of CF lung disease is also seriously questioned by the recent findings that patients with a loss of TMEM16A-function also lack CFTR function [39]. Yet, these patients do not develop any lung disease. Similarly, mice that lack of TMEM16A in ciliated epithelial cells also lack CFTR function [3, 4]. Again, these mice do not develop a lung disease, although they even show a lower intratracheal pH (Fig. 8b). In contrast, in both open and short circuited Ussing chamber measurements and in the absence or presence of bicarbonate, we found

Fig. 8 Calibration curve and pH values in mouse trachea. **a** Calibration curve for the microelectrode used in airway pH measurements ($n = 3$ measurements each). **b** pH measured in tracheas of T16A$^{flox/flox}$ wild-type mice and mice with a knockout of TMEM16A in ciliated airway epithelial cells (T16A$^{flox/flox}$-FoxJ1Cre). Mean ± SEM (number of animals/number of pooled measurements). #Significant difference when compared with T16A$^{flox/flox}$ ($p < 0.05$, unpaired t-test)
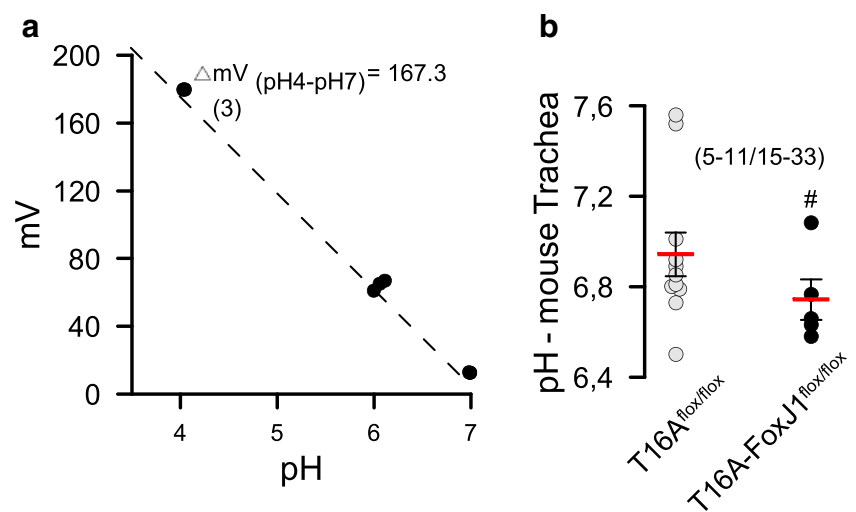
evidence for enhanced amiloride-sensitive Na$^+$ transport in primary CF airway epithelia (Figs. 5 and 6). This is in contrast to data reported from another CF porcine model [22], but is in line with many previous measurements obtained ex vivo in human respiratory tissues, primary airway epithelial cells, and CF intestine [30]. Taken together, the present data question the pathogenic role of defective CFTR-dependent ion transport and acidic pH in CF, but rather suggest that intrinsic airway inflammation along with Na$^+$ hyperabsorption is the cause for CF lung disease.

Compliance with ethical standards

Conflict of interest The authors declare that they have no conflict of interest.

References

1. Ballard ST, Trout L, Mehta A, Inglis SK (2002) Liquid secretion inhibitors reduce mucociliary transport in glandular airways. Am J Phys Lung Cell Mol Phys 283:L329–L335

2. Benedetto R, Cabrita I, Schreiber R, Kunzelmann K (2019) TMEM16A is indispensable for basal mucus secretion in airways and intestine. FASEB J 33:4502–4512

3. Benedetto R, Ousingsawat J, Cabrita I, Pinto M, Lerias J, Wanitchakool P, Schreiber R, Kunzelmann K (2019) Plasma membrane localized TMEM16 proteins are indispensable for expression of CFTR. J Mol Med 97:711–722

4. Benedetto R, Ousingsawat J, Wanitchakool P, Zhang Y, Holtzman MJ, Amaral M, Rock JR, Schreiber R, Kunzelmann K (2017) Epithelial chloride transport by CFTR requires TMEM16A. Sci Rep 7:12397

5. Billet A, Hanrahan JW (2013) The secret life of CFTR as a calcium-activated chloride channel. J Physiol 591:5273–5278

6. Boucher RC, Stutts MJ, Knowles MR, Cantley L, Gatzy JT (1986) Na+ transport in cystic fibrosis respiratory epithelia: abnormal basal rate and response to adenylate cyclase. J Clin Invest 78:1245–1252

7. Cabrita I, Benedetto R, Schreiber R, Kunzelmann K (2019) Niclosamide repurposed for the treatment of inflammatory airway disease. JCI Insight 8:128414

8. Chen JH, Stoltz DA, Karp PH, Ernst SE, Pezzulo AA, Moninger TO, Rector MV, Reznikov LR, Launspach JL, Chaloner K, Zabner J, Welsh MJ (2010) Loss of anion transport without increased sodium absorption characterizes newborn porcine cystic fibrosis airway epithelia. Cell 143:911–923

9. Cooper JL, Quinton PM, Ballard ST (2013) Mucociliary transport in porcine trachea: differential effects of inhibiting chloride and bicarbonate secretion. Am J Phys Lung Cell Mol Phys 304:L184–L190

10. Fulcher ML, Gabriel S, Burns KA, Yankaskas JR, Randell SH (2005) Well-differentiated human airway epithelial cell cultures. Methods Mol Med 107:183–206

11. Garnett JP, Hickman E, Burrows R, Hegyi P, Tiszlavicz L, Cuthbert AW, Fong P, Gray MA (2011) Novel role for pendrin in orchestrating bicarbonate secretion in cystic fibrosis transmembrane conductance regulator (CFTR)-expressing airway serous cells. J Biol Chem 286:41069–41082

12. Gorrieri G, Scudieri P, Caci E, Schiavon M, Tomati V, Sirci F, Napolitano F, Carrella D, Gianotti A, Musante I, Favia M, Casavola V, Guerra L, Rea F, Ravazzolo R, Di Bernardo D, Galietta LJ (2016) Goblet cell hyperplasia requires high bicarbonate transport to support mucin release. Sci Rep 6:36016

13. Grubb BR, Boucher RC (1999) Pathophysiology of gene-targeted mouse models for cystic fibrosis. Physiol Rev 79:S193–S214

14. Grubb BR, Vick RN, Boucher RC (1994) Hyperabsorption of Na$^+$ and raised Ca^{2+} mediated cl$^-$ secretion in nasal epithelia of CF mice. Am J Phys 266:C1478–C1483

15. Haggie PM, Phuan PW, Tan JA, Zlock L, Finkbeiner WE, Verkman AS (2016) Inhibitors of pendrin anion exchange identified in a small molecule screen increase airway surface liquid volume in cystic fibrosis. FASEB J:fj

16. Han Y, Shewan AM, Thorn P (2016) HCO3- transport through anoctamin/transmembrane protein ANO1/TMEM16A, in pancreatic acinar cells, regulates luminal pH. J Biol Chem 291:20345–20352

17. Hill DB, Long RF, Kissner WJ, Atieh E, Garbarine IC, Markovetz MR, Fontana NC, Christy M, Habibpour M, Tarran R, Gregory Forest M, Boucher RC, Button B (2018) Pathological mucus and impaired mucus clearance in cystic fibrosis patients results from increased concentration, not altered pH. Eur Respir J 52:1801297

18. Hoegger MJ, Fischer AJ, McMenimen JD, Ostedgaard LS, Tucker AJ, Awadalla MA, Moninger TO, Michalski AS, Hoffman EA, Zabner J, Stoltz DA, Welsh MJ (2014) Impaired mucus detachment disrupts mucociliary transport in a piglet model of cystic fibrosis. Science 345:818–822

19. Hug MJ, Bridges RJ (2001) pH regulation and bicarbonate transport of isolated porcine submucosal glands. JOP 2:274–279

20. Hull J, Vervaart P, Grimwood K, Phelan P (1997) Pulmonary oxidative stress response in young children with cystic fibrosis. Thorax 52:557–560

21. Inglis SK, Corboz MR, Ballard ST (1998) Effect of anion secretion inhibitors on mucin content of airway submucosal gland ducts. Am J Phys 274:L762–L766

22. Itani OA, Chen JH, Karp PH, Ernst S, Keshavjee S, Parekh K, Klesney-Tait J, Zabner J, Welsh MJ (2011) Human cystic fibrosis airway epithelia have reduced cl- conductance but not increased Na+ conductance. Proc Natl Acad Sci U S A 108:10260–10265

23. Jayaraman S, Song Y, Vetrivel L, Shankar L, Verkman AS (2001) Noninvasive in vivo fluorescence measurement of airway-surface liquid depth, salt concentration, and pH. J Clin Invest 107:317–324

24. Joo NS, Cho HJ, Khansaheb M, Wine JJ (2010) Hyposecretion of fluid from tracheal submucosal glands of CFTR-deficient pigs. J Clin Invest 120:3161–3166

25. Joo NS, Saenz Y, Krouse ME, Wine JJ (2002) Mucus secretion from single submucosal glands of pig. Stimulation by carbachol and vasoactive intestinal peptide. J Biol Chem 277:28167–28175

26. Jung J, Nam JH, Park HW, Oh U, Yoon JH, Lee MG (2012) Dynamic modulation of ANO1/TMEM16A HCO3- permeability by Ca2+/calmodulin. Proc Natl Acad Sci USA

27. Kim D, Huang J, Billet A, Abu-Arish A, Goepp J, Matthes E, Tewfik MA, Frenkiel S, Hanrahan JW (2019) Pendrin mediates bicarbonate secretion and enhances CFTR function in airway surface epithelia. Am J Respir Cell Mol Biol 60:705–716

28. Klymiuk N, Mundhenk L, Kraehe K, Wuensch A, Plog S, Emrich D, Langenmayer MC, Stehr M, Holzinger A, Kroner C, Richter A, Kessler B, Kurome M, Eddicks M, Nagashima H, Heinritzi K, Gruber AD, Wolf E (2012) Sequential targeting of CFTR by BAC vectors generates a novel pig model of cystic fibrosis. J Mol Med (Berl) 90:597–608

29. Kunzelmann K, Centeio R, Wanitchakool P, Cabrita I, Benedetto R, Saha T, Hoque KM, Schreiber R (2019) Control of ion transport by Tmem16a expressed in murine intestine. Front Physiol 10:1262

30. Kunzelmann K, Ousingsawat J, Cabrita I, Doušová T, Bähr A, Janda M, Schreiber R, Benedetto R (2019) TMEM16A in cystic fibrosis: activating or inhibiting? Front Pharmacol 29(10):3

31. Lerias J, Pinto M, Benedetto R, Schreiber R, Amaral M, Aureli M, Kunzelmann K (2018) Compartmentalized crosstalk of CFTR and TMEM16A (ANO1) through EPAC1 and ADCY1. Cell Signal 44: 10–19

32. Liu J, Walker NM, Ootani A, Strubberg AM, Clarke LL (2015) Defective goblet cell exocytosis contributes to murine cystic fibrosis-associated intestinal disease. J Clin Invest 125:1056–1068

33. Mall M, Bleich M, Greger R, Schreiber R, Kunzelmann K (1998) The amiloride inhibitable Na$^+$ conductance is reduced by CFTR in normal but not in CF airways. J Clin Invest 102:15–21

34. Mall M, Bleich M, Greger R, Schürlein M, Kühr J, Seydewitz HH, Brandis M, Kunzelmann K (1998) Cholinergic ion secretion in human colon requires co-activation by cAMP. Am J Phys 275: G1274–G1281

35. McConnell EL, Basit AW, Murdan S (2008) Measurements of rat and mouse gastrointestinal pH, fluid and lymphoid tissue, and implications for in-vivo experiments. J Pharm Pharmacol 60:63–70

36. Meyerholz DK, Stoltz DA, Namati E, Ramachandran S, Pezzulo AA, Smith AR, Rector MV, Suter MJ, Kao S, McLennan G, Tearney GJ, Zabner J, McCray PB Jr, Welsh MJ (2010) Loss of CFTR function produces abnormalities in tracheal development in neonatal pigs and young children. Am. J Respir. Crit Care Med 182: 1251–1261

37. Namkung W, Finkbeiner WE, Verkman AS (2010) CFTR-adenylyl cyclase I association is responsible for UTP activation of CFTR in well-differentiated primary human bronchial cell cultures. Mol Biol Cell 21:2639–2648

38. Ostedgaard LS, Meyerholz DK, Chen JH, Pezzulo AA, Karp PH, Rokhlina T, Ernst SE, Hanfland RA, Reznikov LR, Ludwig PS, Rogan MP, Davis GJ, Dohrn CL, Wohlford-Lenane C, Taft PJ, Rector MV, Hornick E, Nassar BS, Samuel M, Zhang Y, Richter SS, Uc A, Shilyansky J, Prather RS, McCray PB, Jr., Zabner J, Welsh MJ, Stoltz DA (2011) The {Delta}F508 mutation causes CFTR misprocessing and cystic fibrosis-like disease in pigs. Sci. Transl. Med 3:74ra24

39. Park JH, Ousingsawat J, Cabrita I, Bettels RE, Große-Onnebrink J, Schmalstieg C, Biskup S, Reunert J, Rust S, Schreiber R, Kunzelmann K, Marquardt T (2020) TMEM16A deficiency: a potentially fatal neonatal disease resulting from impaired chloride currents. J Med Genet:jmedgenet-2020-106978

40. Pezzulo AA, Tang XX, Hoegger MJ, Alaiwa MH, Ramachandran S, Moninger TO, Karp PH, Wohlford-Lenane CL, Haagsman HP, van Eijk M, Banfi B, Horswill AR, Stoltz DA, McCray PB Jr, Welsh MJ, Zabner J (2012) Reduced airway surface pH impairs bacterial killing in the porcine cystic fibrosis lung. Nature 487:109–113

41. Rogers CS, Stoltz DA, Meyerholz DK, Ostedgaard LS, Rokhlina T, Taft PJ, Rogan MP, Pezzulo AA, Karp PH, Itani OA, Kabel AC, Wohlford-Lenane CL, Davis GJ, Hanfland RA, Smith TL, Samuel M, Wax D, Murphy CN, Rieke A, Whitworth K, Uc A, Starner TD, Brogden KA, Shilyansky J, McCray PB Jr, Zabner J, Prather RS, Welsh MJ (2008) Disruption of the CFTR gene produces a model of cystic fibrosis in newborn pigs. Science 321:1837–1841

42. Rosenow T, Mok LC, Turkovic L, Berry LJ, Sly PD, Ranganathan S, Tiddens H, Stick SM (2019) The cumulative effect of inflammation and infection on structural lung disease in early cystic fibrosis. Eur Respir J 54:1801771

43. Rottner M, Tual-Chalot S, Mostefai HA, Andriantsitohaina R, Freyssinet JM, Martinez MC (2011) Increased oxidative stress induces apoptosis in human cystic fibrosis cells. PLoS One 6:e24880

44. Saint-Criq V, Haq IJ, Gardner AI, Garnett JP, Ward C, Brodlie M, Gray MA (2019) Real-time, semi-automated fluorescent measurement of the airway surface liquid pH of primary human airway epithelial cells. J Vis Exp

45. Scholte BJ, Horati H, Veltman M, Vreeken RJ, Garratt LW, Tiddens H, Janssens HM, Stick SM (2019) Oxidative stress and abnormal bioactive lipids in early cystic fibrosis lung disease. J Cyst Fibros 18:781–789

46. Schreiber R, Buchholz B, Kraus A, Schley G, Scholz J, Ousingsawat J, Kunzelmann K (2019) Lipid peroxidation drives renal cyst growth in vitro through activation of TMEM16A. J Am Soc Nephrol 30:228–242

47. Schultz A, Puvvadi R, Borisov SM, Shaw NC, Klimant I, Berry LJ, Montgomery ST, Nguyen T, Kreda SM, Kicic A, Noble PB, Button B, Stick SM (2017) Airway surface liquid pH is not acidic in children with cystic fibrosis. Nat Commun 8:1409

48. Schutte A, Ermund A, Becker-Pauly C, Johansson ME, Rodriguez-Pineiro AM, Backhed F, Muller S, Lottaz D, Bond JS, Hansson GC (2014) Microbial-induced meprin beta cleavage in MUC2 mucin and a functional CFTR channel are required to release anchored small intestinal mucus. Proc Natl Acad Sci U S A 111:12396–12401

49. Shah VS, Meyerholz DK, Tang XX, Reznikov L, Abou AM, Ernst SE, Karp PH, Wohlford-Lenane CL, Heilmann KP, Leidinger MR, Allen PD, Zabner J, McCray PB Jr, Ostedgaard LS, Stoltz DA, Randak CO, Welsh MJ (2016) Airway acidification initiates host defense abnormalities in cystic fibrosis mice. Science 351:503–507

50. Simonin J, Bille E, Crambert G, Noel S, Dreano E, Edwards A, Hatton A, Pranke I, Villeret B, Cottart CH, Vrel JP, Urbach V, Baatallah N, Hinzpeter A, Golec A, Touqui L, Nassif X, Galietta LJV, Planelles G, Sallenave JM, Edelman A, Sermet-Gaudelus I (2019) Airway surface liquid acidification initiates host defense abnormalities in cystic fibrosis. Sci Rep 9:6516

51. Stoltz DA, Meyerholz DK, Pezzulo AA, Ramachandran S, Rogan MP, Davis GJ, Hanfland RA, Wohlford-Lenane C, Dohrn CL, Bartlett JA, Nelson GA, Chang EH, Taft PJ, Ludwig PS, Estin M, Hornick EE, Launspach JL, Samuel M, Rokhlina T, Karp PH, Ostedgaard LS, Uc A, Starner TD, Horswill AR, Brogden KA, Prather RS, Richter SS, Shilyansky J, McCray PB Jr, Zabner J, Welsh MJ (2010) Cystic fibrosis pigs develop lung disease and exhibit defective bacterial eradication at birth. Sci Transl Med 2:29ra31

52. Verhaeghe C, Delbecque K, de Leval L, Oury C, Bours V (2007) Early inflammation in the airways of a cystic fibrosis foetus. J Cyst Fibros 6:304–308

53. Wilke M, Buijs-Offerman RM, Aarbiou J, Colledge WH, Sheppard DN, Touqui L, Bot A, Jorna H, De Jonge HR, Scholte BJ (2011) Mouse models of cystic fibrosis: phenotypic analysis and research applications. J Cyst Fibros 10(Suppl 2):9